NASA Technical Paper 2297

April 1984

Experimental Investigation of Tangential Blowing Applied to a Subsonic V/STOL Inlet

Richard R. Burley

NASA

NASA
Technical
Paper
2297

1984

Experimental Investigation of Tangential Blowing Applied to a Subsonic V/STOL Inlet

Richard R. Burley

Lewis Research Center
Cleveland, Ohio

NASA
National Aeronautics
and Space Administration

Scientific and Technical
Information Branch

Summary

Engine inlets for subsonic V/STOL aircraft must operate over a wide range of conditions without the severe internal flow separation that can cause sudden changes in engine thrust, excessively high fan blade stresses, and possibly core-compressor stall. An experimental investigation was conducted to evaluate the effectiveness of tangential blowing to maintain attached flow at high inlet angles of attack. The inlet had a relatively thin lip (lip contraction ratio of 1.46). Two blowing slot locations were investigated: one on the lip and the other in the diffuser. The effect of two slot heights (0.0508 and 0.152 cm) and three slot circumferential extents, the largest being 120°, also was investigated.

The results showed that both lip and diffuser blowing were effective in maintaining attached flow at high angles of attack. However, higher angle-of-attack capability was achieved with lip blowing than with diffuser blowing. This capability was achieved with the largest slot circumferential extent and either of the two slot heights.

The tests were conducted in a low-speed wind tunnel at free-stream velocities between 18 and 62 m/sec and inlet angles of attack to 110°. Inlet throat Mach number varied between 0.15 and 0.60. Blowing pressure ratio (blowing total pressure divided by free-stream total pressure) was varied between 1.0 and 1.4. Blowing temperature ratio (blowing total temperature divided by free-stream total temperature) was nominally 1.0.

Introduction

Engine inlets for tilt-nacelle subsonic V/STOL aircraft must operate efficiently over a wide range of flight speeds, engine throttle settings, and inlet angles of attack. Studies indicate that these inlets can experience angles of attack as high as 120° at flight speeds of 21 m/sec. A major concern of the designer in maintaining efficient engine operation at these severe conditions is possible inlet internal boundary layer separation. Separation-free flow is desirable to minimize both engine thrust losses and fan blade stresses.

The NASA Lewis Research Center currently is engaged in a research program to evaluate the effectiveness of a wide variety of techniques to help prevent flow separation within the inlets of V/STOL aircraft. The emphasis so far has been on examining geometric techniques applicable to subsonic V/STOL aircraft. The major ones include lip thickness for both symmetric (refs. 1 to 9) and asymmetric (refs. 10 and 11) inlets, inlets that have a protruding lower lip (refs. 12 to 14), and inlets with extended centerbodies (refs. 9, 15, and 16).

Another technique that can be used to prevent internal flow separation is to blow a thin jet of high-pressure air tangentially into the boundary layer to reenergize it. Blowing is attractive because high-pressure air is readily available from the core compressor. Results where blowing was used for inlet boundary layer control have been published in reference 17. The blowing slot was located in the diffuser of an inlet with a thick lower lip.

The present study used an inlet with a relatively thin lip and evaluated the effectiveness of blowing at each of two locations: either on the lip or in the diffuser. The effect of two slot heights (0.0508 and 0.152 cm) and three slot circumferential extents, the largest being 120°, also was investigated. The inlet contraction ratio (highlight- to throat-area ratio) was 1.46.

The tests were conducted in the Lewis Research Center's 9- by 15-Foot Low-Speed Wind Tunnel. The inlet was sized to fit a 50.8-cm-diameter fan simulator. Data were taken over a range of free-stream velocities from 18 to 62 m/sec and angles of attack to 110°. Inlet throat Mach number was varied between 0.15 and 0.60. Blowing pressure ratio (blowing total pressure divided by free-stream total pressure) was varied between 1.0 and 1.4. Blowing temperature ratio (blowing total temperature divided by free-stream total temperature) was constant at about 1.0.

Symbols

A	area
a	major axis of elliptical internal lip (fig. 2)
b	minor axis of elliptical internal lip (fig. 2)
CR	internal lip contraction ratio
c	external forebody length (fig. 2)
D	diameter
d	external forebody thickness (fig. 2)

h blowing slot height (fig. 2)
L inlet length
LW leeward plane
m weight flow
P total pressure
p static pressure
Re Reynolds number
RBP relative blowing power
T total temperature
V velocity
WW windward plane
x axial distance from inlet highlight
y radial distance from inlet highlight
z boundary layer rake height
α angle of attack
γ ratio of specific heats
θ circumferential extent of blowing (fig. 2)
λ_{max} maximum diffuser wall angle (fig. 2)
σ fan blade vibratory stress
φ circumferential position (fig. 3)

Subscripts:

b blowing
c centerbody
d diffuser
e diffuser exit
f fan
i inlet
h inlet highlight
l lip
max maximum
t inlet throat
0 free stream

Apparatus and Procedure

Test Model

A schematic of the inlet-fan assembly is shown in figure 1. The fan is a single-stage 50.8-cm-diameter design with 15 rotor blades and 25 stator blades. At the design rotational speed of 8020 rpm the fan pressure ratio is about 1.17 and the tip speed is 213.5 m/sec. The fan is driven by a four-stage turbine powered by high-pressure, heated air delivered to the turbine through flow passages in the model support strut. The model fan design is described more completely in reference 18.

The baseline (i.e., nonblowing) inlet configuration is shown in figure 2(a), and the design parameters are listed in table I. The inlet is a symmetric design with a lip contraction ratio A_h/A_t of 1.46. This results in a rela-

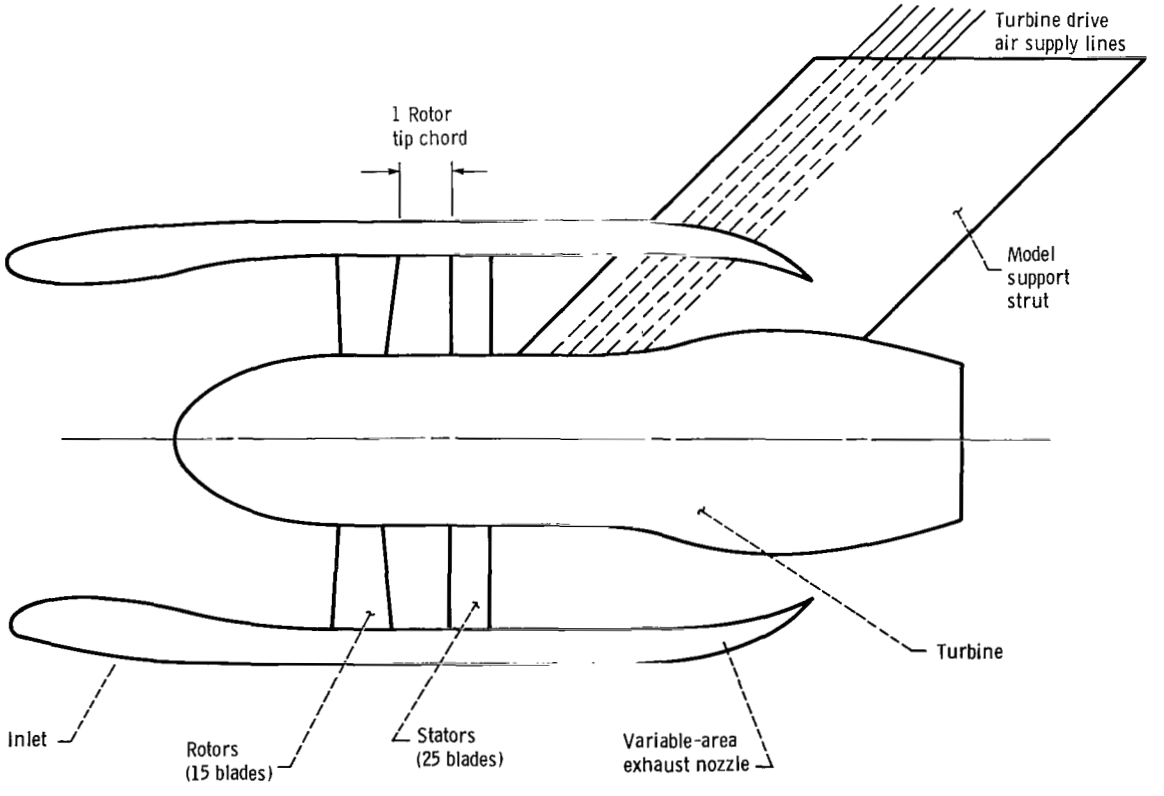

Figure 1. – Inlet-fan assembly.

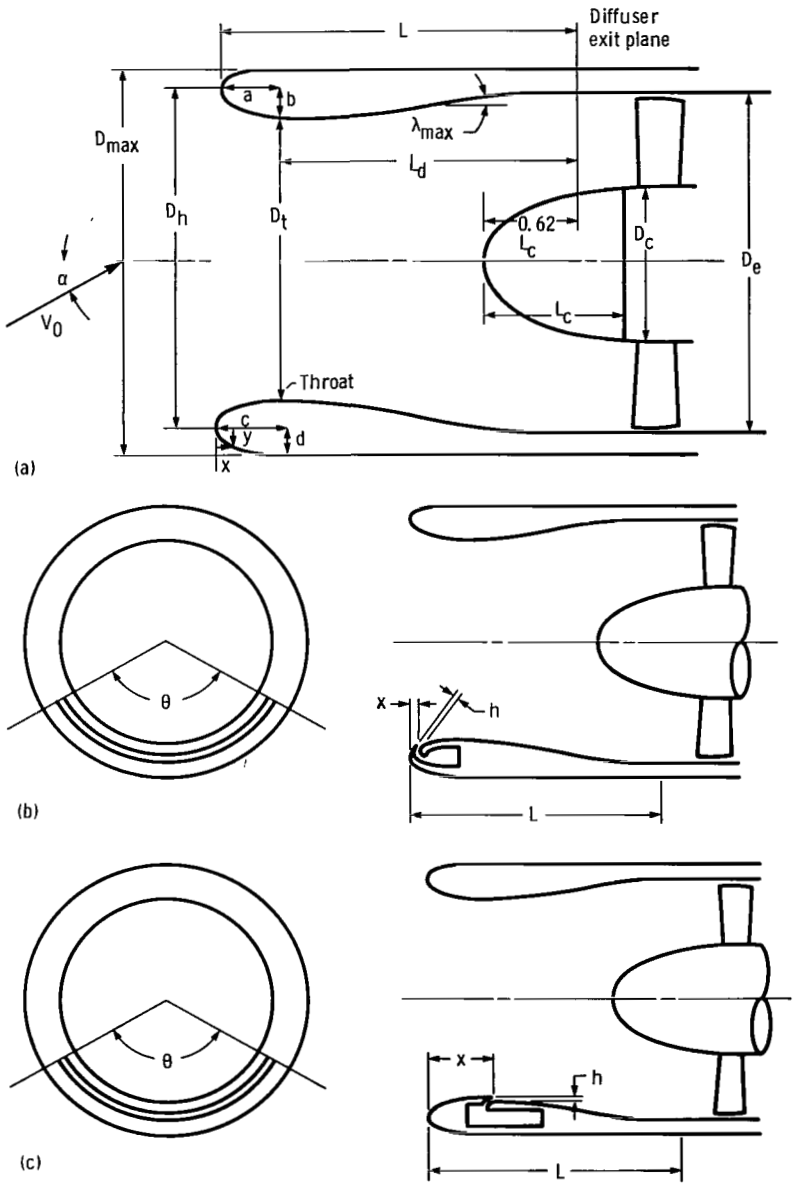

(a) Baseline.
(b) Lip blowing.
(c) Diffuser blowing.

Figure 2. – Inlet configurations.

tively thin-lip inlet for subsonic V/STOL applications, where contraction ratios of 1.69 and 1.76 have been suggested (refs. 19 and 10, respectively). The internal lip shape is elliptic with a major- to minor-axis ratio a/b of 2.0. The diffuser has a cubic shape with a maximum wall angle λ_{max} of 8.7 ocurring halfway down the diffuser. The external forebody has a DAC-1 contour and was designed for a drag divergence Mach number of about 0.79. The overall ratio of inlet length to fan diameter is 1.029.

The centerbody was designed to be compatible with the fan. Its design parameters also are listed in table I.

The blowing inlet configurations are shown in figures 2(b) and (c) and the slot geometric variables are listed in table II. The slots were centered on the windward plane of the inlet ($\varphi = 0°$) and were designed to discharge the blowing air tangent to the wall surface. These were convergent slots that had a short parallel length section at the exit to ensure that the jet was directed properly. The slot was continuous (as opposed to a series of discrete

TABLE I. – INLET GEOMETRIC PARAMETERS

Internal lip	
Contraction ratio, $(D_h/D_t)^2$	1.46
Surface contour	Ellipse
Proportions, a/b	2.0
External forebody	
Diameter ratio, D_h/D_{max}	0.900
Ratio of length to maximum diameter, c/D_{max}	0.219
Surface contour[a]	DAC-1
Proportions, c/d	4.380
Diffuser	
Ratio of exit flow area to inlet flow area, $(D_e^2-D_c^2)/D_t^2$	1.156
Ratio of diffuser length to exit diameter, L_d/D_e	0.856
Maximum local wall angle, λ_{max}, deg	8.7
Location of maximum local wall angle, percent L_d	50
Equivalent conical half-angle, deg	2.08
Surface contour	Cubic
Centerbody	
Ratio of length to diameter, L_c/D_c	0.935
Surface contour	NACA-1
Ratio of centerbody length to diffuser length, L_c/L_d	0.418
Ratio of centerbody diameter to diffuser-exit diameter, D_c/D_e	0.46
Overall	
Ratio of inlet length to diffuser-exit diameter, L/D_e	1.029

[a]The DAC-1 contour was developed by the Douglas Aircraft Co. and is given by $(y/d)^2 = 2.318(x/c) - 2.748(x/c)^2 + 2.544(x/c)^3 - 1.113(x/c)^4$.

TABLE II. – BLOWING GEOMETRIC PARAMETERS

Location	Fractional distance from highlight, x/L	Blowing slot height, h, cm	Circumferential extent of blowing, θ, deg
Lip	0.008	0.0508	120
		.0508	60
		.0508	30
		.152	120
		.152	90
		.152	60
Diffuser	.20	.0508	120
	.20	.152	120

nozzles), as this has been shown to work well for wing blowing (ref. 20). Two slot locations were investigated: one on the lip and the other in the diffuser. The lip slot, shown in figure 2(b), was located as close to the inlet highlight (leading edge) as practical ($x/L = 0.008$). Both the height and circumferential extent of this slot were varied. A 0.0508-cm-high slot was tested at circumferential extents of 30°, 60°, and 120°, and a 0.152-cm-high slot was tested at circumferential extents of 60°, 90°, and 120°. The diffuser slot, shown in figure 2(c), was located as close to the inlet throat as practical ($x/L = 0.20$). (The inlet throat is at $x/L = 0.17$.) The two diffuser slot heights tested were the same as those for the lip slot (0.0508 and 0.152 cm). The circumferential extent of the diffuser slot, however, was held constant at 120°.

Instrumentation

The aerodynamic instrumentation is shown in figure 3(a). Axial rows of static pressure taps, extending from the highlight to the diffuser exit, were located on the internal surface of the inlet at two circumferential locations. For this report only the windward plane distribution ($\varphi = 0°$) is presented since the most severe flow conditions occur there. One six-tube boundary layer total pressure rake was located in the diffuser ($x/L = 0.25$) slightly downstream of the throat and 5° from the windward plane. (The boundary layer rake was just downstream of the diffuser blowing slot located at $x/L = 0.20$.) Eight equally spaced total pressure rakes, each containing 19 total pressure tubes, were located at the fan face. Six tubes on each rake were positioned to provide an equal-area-weighted measurement of the fan

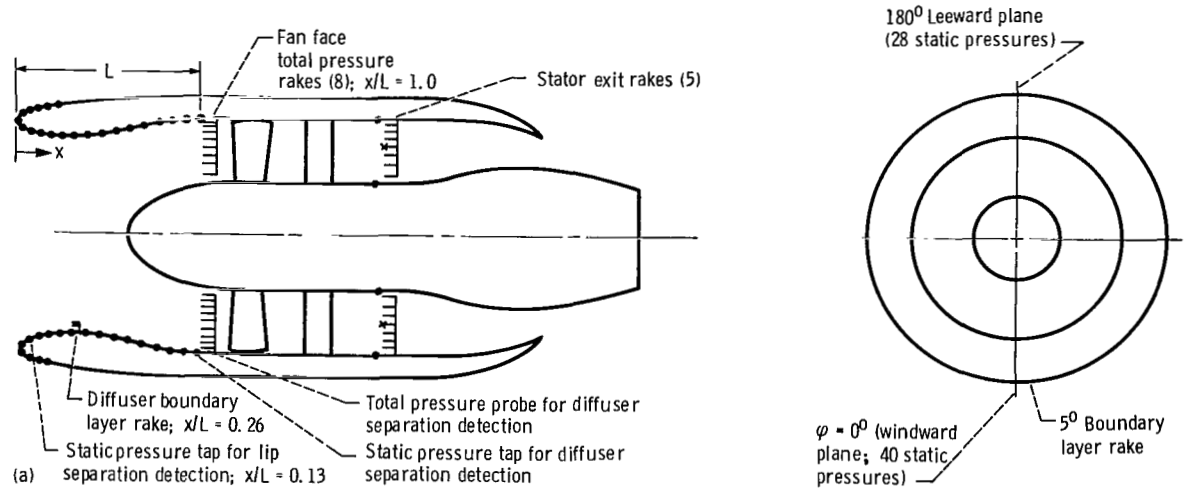

(a)

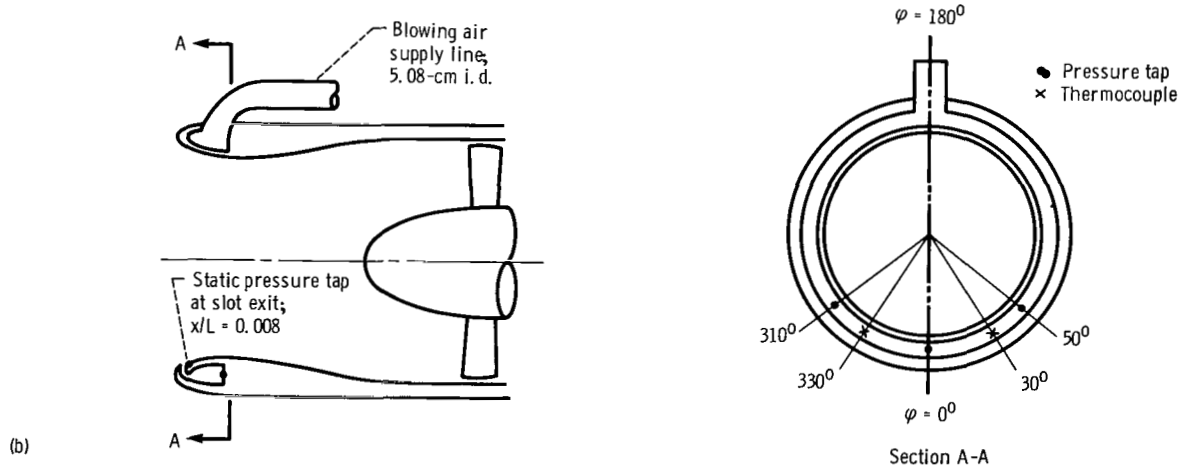

(b)

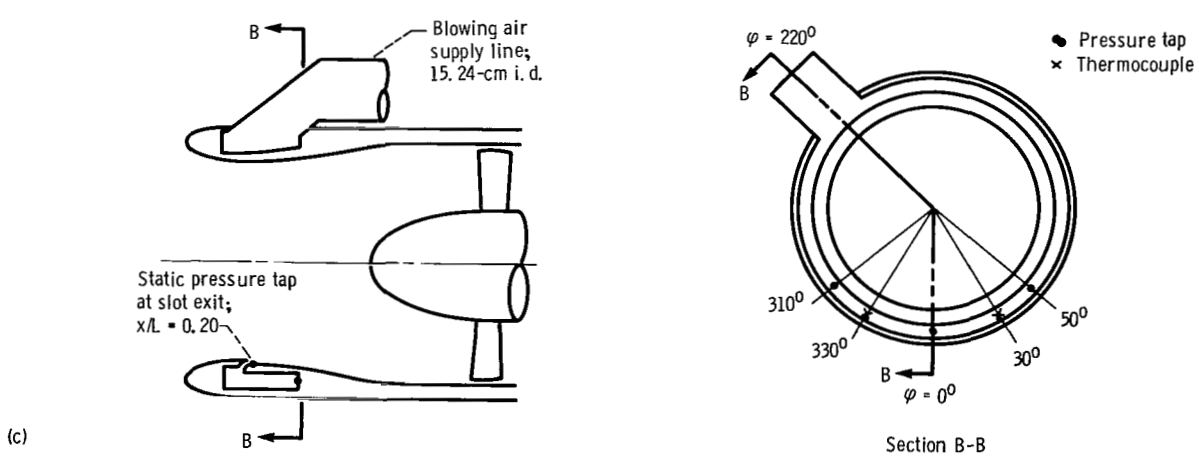

(c)

(a) Aerodynamic.
(b) Lip blowing.
(c) Diffuser blowing.

Figure 3. – Instrumentation.

face total pressure. The remaining tubes were positioned to provide a more detailed measurement of the outer surface boundary layer and midchannel flow. Five equally spaced rakes with six total pressure tubes and one thermocouple per rake were located downstream of the fan stators.

Inlet internal flow separation was detected from a measurement of both static pressure on the lip (for lip separation) and total minus static pressure at the diffuser exit (for diffuser separation) as shown in figure 3(a). The measurements were monitored continuously during the test. This technique for detecting internal flow separation is detailed in reference 9.

The fan blade vibratory stress was measured with a strain gage located at the root on the suction side of one of the blades. This position was responsive to the first bending mode of the blade, which had previously been determined to be the only significant mode of vibration (ref. 11). The strain-gage signal was monitored continuously during the test on an x-y plotter.

The blowing instrumentation is shown in figures 3(b) and (c) for lip and diffuser blowing, respectively. Three equally spaced pressure taps, located in the plenum chamber as far removed from the slot exit as possible, provided the measurement of blowing total pressure. Two equally spaced thermocouples, located in the same plane as the pressure taps, provided the measurement of blowing total temperature. A static pressure tap, located at the slot exit, provided the measurement of blowing static pressure. This was used along with the measurements of total pressures and temperatures to calculate the isentropic jet velocity of the blowing air.

The blowing mass flow rate was determined with calibrated choked-flow venturis. The blowing air was supplied from the same source of high-pressure heated air that was used to power the simulator. For lip blowing (fig. 3(b)) the air was delivered to the inlet plenum chamber through a 5.08-cm-i.d. flexible line attached to the leeward side ($\varphi = 180°$) of the inlet. For diffuser blowing (fig. 3(c)) the air was delivered to the inlet plenum chamber through a 15.24-cm-i.d. flexible line attached to the inlet at $\varphi = 220°$. This second line was large because it was originally sized to provide for boundary layer suction.

Test Facility

The tests were conducted in the Lewis Research Center's 9- by 15-Foot Low-Speed Wind Tunnel, which is an atmospheric total pressure facility with a free-stream velocity range to 75 m/sec. The facility is described in more detail in reference 21.

The model installed in the test section is shown in figures 4(a) and (b) for lip and diffuser blowing configurations, respectively. To vary angle of attack, the model rotates in a horizontal plane about a vertical support post. The post also provides a passage for the high-pressure turbine drive air, which comes up through the tunnel floor. A vertical pipe that comes down through the tunnel ceiling and is mounted on a swivel joint provides a passage for the high-pressure blowing air. A portion of the adjacent wind tunnel vertical wall was removed to allow the fan and turbine exhaust to pass outside the test section during high-angle-of-attack operation.

Procedure

A major concern during the test was the safety of the fan, which meant that the fan blade stresses should not exceed their limiting value. The procedure for insuring this is detailed in reference 11. Essentially it consisted of first setting a low free-stream velocity and angle of attack with the fan operating at a low speed ($\sim$2000 rpm). Then a "safety sweep" of fan speed was made during which time the inlet passed from a worse condition to a better condition (i.e., from separated to attached flow). The sweep consisted of increasing the fan speed to about 6500 rpm (corresponding to the upper value of throat velocity associated with landing transition maneuvers of subsonic V/STOL aircraft) while continuously monitoring blade stress levels to assure that they remained below their limiting value.

Once the safety sweep had established that the fan blade stresses remained below their limiting value, fan speed was decreased slowly until flow separation was detected by the on-line separation indicators previously discussed. Then data were taken just before and after separation. Additional data were taken to document inlet performance with increasingly severe degrees of separation as well as with attached flow.

At each free-stream velocity the incidence angle was increased in increments of 15° beginning with $\alpha = 0°$, and the above procedure was repeated until either the limiting value of blade stress or the desired incidence angle was reached. This process then was repeated for higher free-stream velocities. In this manner the envelope of safe operating conditions for the baseline inlet was established.

This same operating envelope also was adhered to for the blowing tests. Thus, if some unforeseen event shut off the blowing air supply during the test, fan blade stresses would still remain below the limiting value. The procedure for the blowing test was the same as that for the nonblowing tests with the exception that blowing pressure ratio was set along with free-stream velocity and angle of attack. Note that using the same operating envelope for the blowing tests as for the nonblowing tests meant that sometimes the separation boundary for the blowing configuration was not achieved because the upper limit on angle of attack was set by the nonblowing configuration.

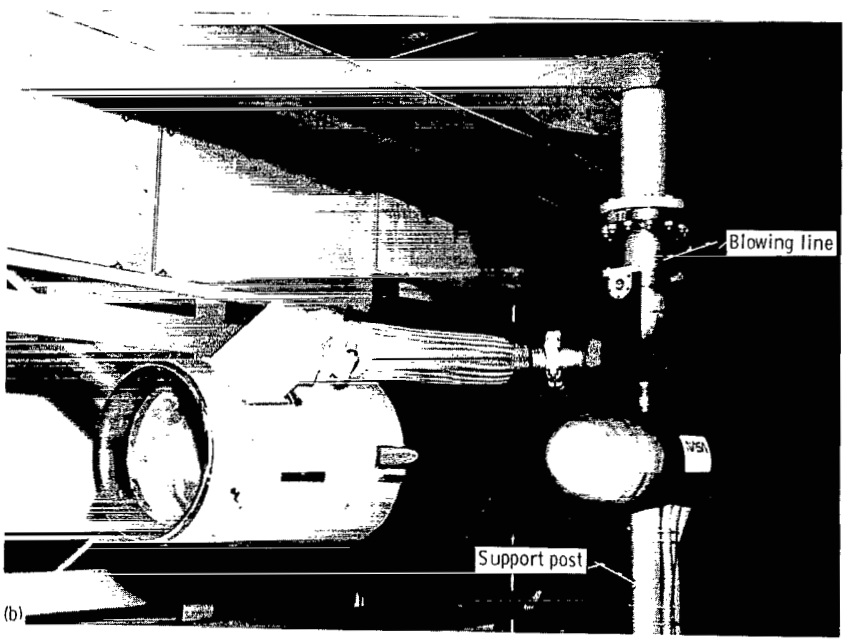

(a) Lip blowing.
(b) Diffuser blowing.

Figure 4. – Inlet fan installed in V/STOL wind tunnel.

Results and Discussion

The first two subdivisions of this section discuss the results of the baseline (nonblowing) inlet. The remaining subdivisions discuss the effect of blowing applied to this inlet.

Separation Behavior of Baseline Inlet

When internal flow separation occurred with the baseline inlet, it propagated instantaneously throughout the entire inlet. This can be seen by examining the behavior of the lip and diffuser separation detectors as a function of engine rotational speed. Traces of this behavior are shown in figures 5(a) and (b) for a free-stream velocity of 18 m/sec and an incidence angle of 110°. As engine rotational speed was decreased, both the lip and diffuser separation indicators showed an abrupt change at the same engine speed (about 6000 rpm), an indication that the flow separation was detected on the lip and in the diffuser at essentially the same time. This type of abrupt separation can result in unacceptably high fan blade stresses. A trace of blade stress level, in terms of the percentage of its maximum value, is shown in figure 5(c) as a function of engine rotational speed. At rotational speeds corresponding to attached flow (above 6000 rpm) the resulting blade stress levels were insignificant. But at rotational speeds corresponding to separated flow (below 6000 rpm) the resulting blade stress levels can be very high. At the rotational speed that resulted in excitation of the first bending mode of vibration by an engine-order-4 disturbance (i.e., a disturbance that resulted in four flatwise bending vibration cycles per revolution), the blade stress level had increased to nearly its maximum value. (See ref. 22 for detailed information on blade stresses induced by flow distortion.)

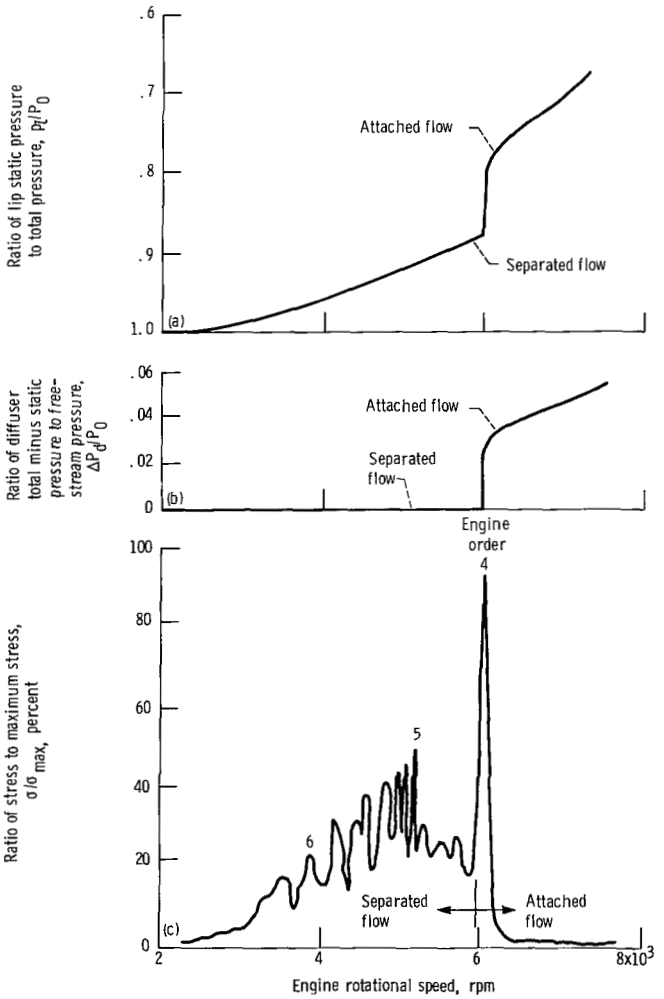

(a) Trace of internal lip static pressure.
(b) Trace of diffuser-exit total minus static pressure ratio.
(c) Fan blade vibratory stress.

Figure 5. – Separation behavior of baseline inlet. Free-stream velocity, V_0, 18 m/sec; angle of attack, α, 110°.

Nonblowing Correlating Parameter

A parameter for correlating the separation bounds for the baseline inlet as well as for any inlet without blowing is described here. This parameter is the ratio of inlet throat velocity to free-stream velocity V_t/V_0. How well it correlates the data for the baseline inlet (no slot) is shown in figure 6. The results are presented in terms of the angle of attack at which flow separation occurs as a function of V_t/V_0 for a range of free-stream velocities that might be encountered during the takeoff and landing maneuvers of V/STOL aircraft.

As can be seen from figure 6, the velocity ratio successfully correlates the results for the baseline inlet. The dashed curve in the figure represents the flow separation

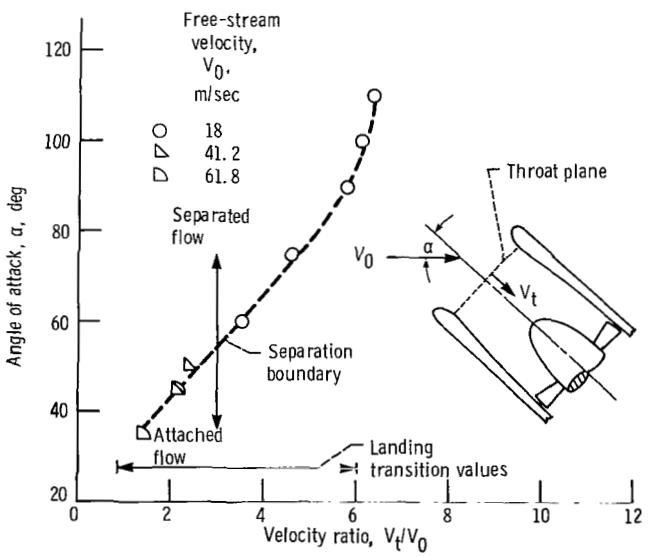

Figure 6. – Flow separation boundaries for baseline (no slot) configuration.

boundary for the inlet. Below the curve the flow is attached; above the curve the flow is separated. This correlating parameter also has been successfully applied to other inlet geometries without boundary layer control devices (ref. 11). Moreover, as shown later, this parameter also correlates the results for inlet configurations that have the blowing slot closed. It should be noted that for all of the results in this report the inlet maximum internal surface velocity was always subsonic (no shocks). This is an important point because the V_t/V_0 correlating parameter is applicable only as long as no shocks are present in the internal flow (ref. 6).

Also shown on the abscissa of figure 6 is a range of values for the velocity ratio that might be encountered during the landing transition of a tilt-nacelle VTOL aircraft (ref. 19). At the start of this transition maneuver the fan is at part throttle (i.e., the throat velocity is low) because the thrust has been reduced to decrease the aircraft speed from cruise conditions. During the landing transition maneuver the aircraft continues to slow down, but the throat velocity now increases as the aircraft transitions from wingborne to thrust-supported operation. The combination of an increase in throat velocity and a decrease in free-stream velocity results in an increase in velocity ratio during this maneuver. According to reference 19, the velocity ratio could increase from 0.85 to 6.0.

Effect of Blowing Location

The effect of blowing slot location (i.e., on the lip or in the diffuser) on the flow separation boundary is shown in figure 7 for a blowing slot height of 0.0508 cm and a slot circumferential extent of 120°. Results are shown in figure 7(a) at a blowing pressure ratio P_b/P_0 of 1.0; in figure 7(b) at a P_b/P_0 of 1.2; and in figure 7(c) at a P_b/P_0 of 1.4. The open symbols denote data points for lip blowing, and the solid symbols denote data points for diffuser blowing. It should be noted that a blowing pressure ratio of 1.0 (i.e., when blowing total pressure is equal to free-stream total pressure) does denote blowing since the static pressure at the exit of the blowing slot is below free-stream total pressure.

As indicated in figure 7, lip and diffuser blowing were effective in maintaining attached flow to high angles of attack. Diffuser blowing (solid symbols) was more effective at the low blowing pressure ratio ($P_b/P_0 = 1.0$, fig. 7(a)). Lip blowing (open symbols) was less effective at this pressure ratio because of the adverse effect of the lip slot itself (as explained later). As blowing pressure ratio increased to 1.2, lip blowing became as effective as diffuser blowing (fig. 7(b)). At the high value of blowing pressure ratio ($P_b/P_0 = 1.4$, fig. 7(c)) lip blowing became more effective than diffuser blowing at high velocity ratios. At this blowing pressure ratio the full benefit of lip blowing at the highest angle of attack as well as both

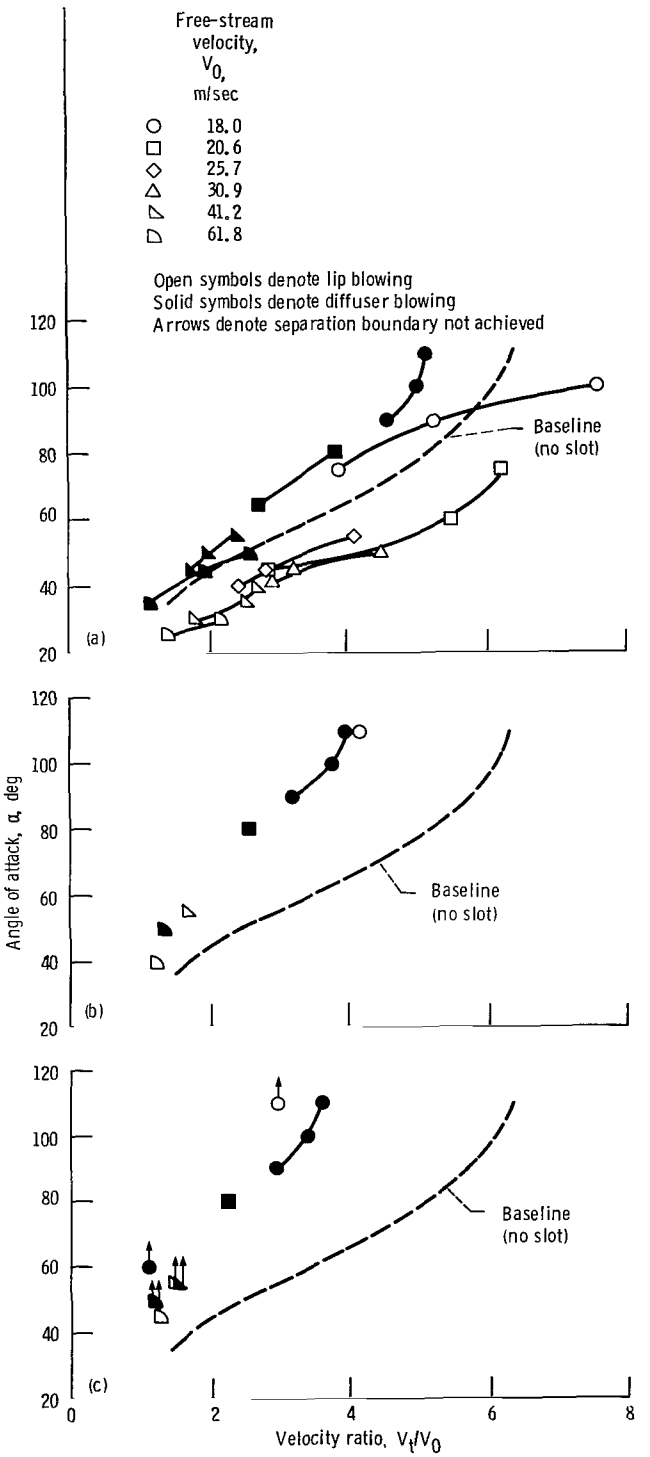

(a) Blowing pressure ratio, P_b/P_0, 1.0.
(b) Blowing pressure ratio, P_b/P_0, 1.2.
(c) Blowing pressure ratio, P_b/P_0, 1.4.

Figure 7. – Effect of blowing location on separation boundary. Lip slot height, h, 0.0508 cm; circumferential extent of blowing, θ, 120°.

lip and diffuser blowing at the low angles of attack could not be demonstrated (symbols with arrow pointing up). The separation boundary could not be determined and still stay within the envelope of safe operating conditions (see discussion of procedure).

The decrease in the effectiveness of diffuser blowing relative to lip blowing with increasing blowing pressure ratio is probably the result of where flow separation is located within the inlet. As the inlet angle of attack is increased with no blowing, separation probably starts in the diffuser and not on the lip. This is inferred from the fact that diffuser blowing is effective and the fact that blowing downstream of where the flow separates generally is not effective (ref. 23). Moreover, analytical results shown in reference 24 indicate that flow separation is located in the diffuser. Hence, the separation must be occurring downstream of the diffuser blowing slot in the inlet diffuser. (Where separation started in the inlet had to be inferred because the slowly responding steady-state measurements of lip and diffuser separation indicated that flow separation on the lip and in the diffuser occurred at essentially the same time.) Applying a sufficiently high diffuser blowing pressure ratio as inlet angle of attack is increased can completely eliminate diffuser separation. At the higher angles of attack, however, further increases in diffuser blowing pressure ratio are not effective because the diffuser is no longer the critical element. Instead, at the higher angles of attack separation occurs on the lip and this, of course, cannot be eliminated by blowing in the diffuser. To eliminate this flow separation problem requires blowing on the lip. And by increasing the lip blowing pressure ratio, inlet angle-of-attack capability can be increased beyond that which can be achieved by diffuser blowing. Moreover, the results in figure 7 indicate that blowing on the lip can eliminate not only lip separation but also diffuser separation. Thus higher angle-of-attack capability can be achieved by lip blowing than by diffuser blowing because at higher angles of attack the separation point moves upstream to the inlet lip.

As previously mentioned, there is an adverse effect of the slot when it is located on the lip but no significant effect when the slot is located in the diffuser. This is shown in figure 8(a), where the flow separation boundaries for the lip-slot-closed configuration (open symbols), the diffuser-slot-closed configuration (solid symbols), and the baseline configuration (i.e., no slot, dashed line) are compared. (The slot was closed in a way that formed a rearward-facing step.) Because the separation boundary for the diffuser-slot-closed configuration is essentially the same as that for the baseline configuration, there is no effect of the diffuser slot. Because the separation boundary for the lip-slot-closed configuration, however, is considerably less than that for the baseline configuration, the lip slot has an adverse effect. The reason for this will be explained shortly.

This same effect accounts for the reduction in the separation boundary with lip blowing at a blowing pressure ratio of 1.0 that was shown in figure 7(a). To further explain this, a comparison is made in figure 8(b) of lip blowing at a blowing pressure ratio of 1.0 with the lip-slot-closed configuration (solid line). Also shown is the baseline configuration (dashed line). The symbols, which denote the lip blowing results, generally have the same separation boundary as the lip-slot-closed configuration. Consequently, lip blowing at this blowing pressure ratio does not reenergize the boundary layer enough to overcome the adverse effect of the lip slot. The result is that lip blowing is not as effective as diffuser blowing at the low blowing pressure ratio.

The adverse effect of the lip slot is composed of two parts. One part can be seen by examining the axial

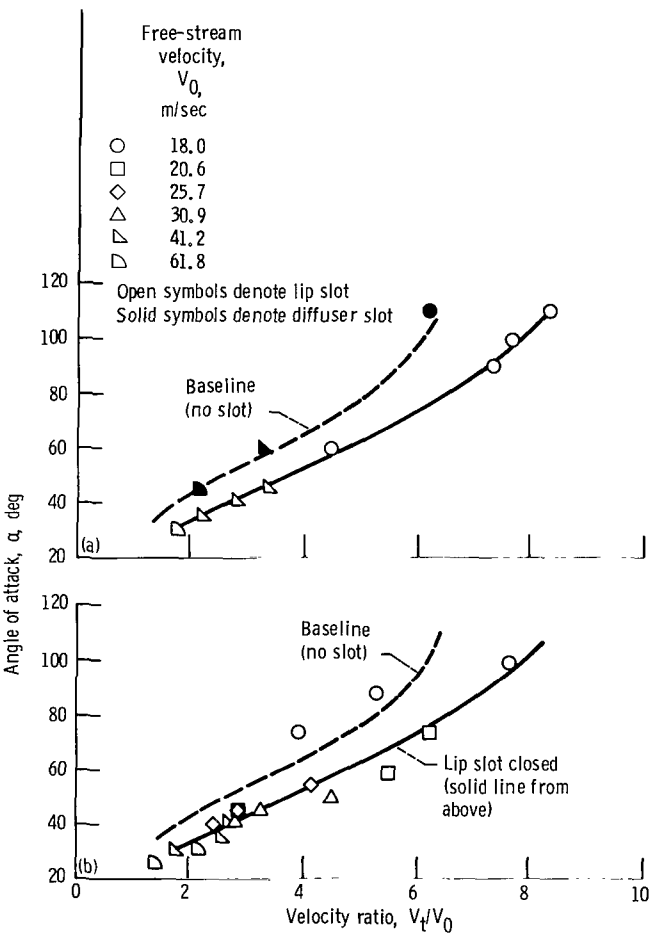

(a) Lip and diffuser slots closed.
(b) Lip blowing pressure ratio, $P_b/P_0 = 1.0$.

Figure 8. – Effect of closed slots on separation boundary and comparison of lip-slot-closed results with lip blowing at a pressure ratio of 1.0. Lip slot height, h, 0.0508 cm; circumferential extent of blowing, θ, 120°.

distribution of internal surface static pressures on the windward side of the inlet. Figure 9 compares this pressure distribution for the baseline configuration and the lip-slot-closed configuration. For both configurations the minimum value of static pressure occurs at the highlight (i.e., at $x/L=0$). The lip-slot-closed configuration, however, has a lower value for this minimum static pressure, which results in an increase in the already steep adverse pressure gradient downstream of the lip slot. This, in turn, increases the tendency of the flow to separate from the lip-slot-closed configuration as compared with the baseline configuration. An increase in the curvature of the lip-slot-closed configuration in the region of the highlight as compared with that of the baseline configuration could be responsible for the observed effect. No such effect was observed for the diffuser-slot-closed configuration.

The other part of the adverse effect of the lip slot is due to the fact that, at the lip slot, the flow separates as it passes over the rearward-facing step formed by the closed slot and then reattaches at some distance downstream. From reference 25, it is reasonable to assume that, at the location where flow reattachment occurs, the boundary layer profile is relatively "weak" as compared with the profile that exists at this location for the baseline configuration. Also, a very steep adverse pressure gradient exists downstream of the lip slot as already mentioned. Consequently, the "weak" profile associated with the lip slot configuration is much more likely to separate because of this steep adverse gradient than is the profile associated with the baseline configuration. Both parts of the adverse effect of the lip slot contribute to the lower separation boundary shown in figure 8(a) for the lip-slot-closed configuration as compared with the separation boundary for the baseline configuration.

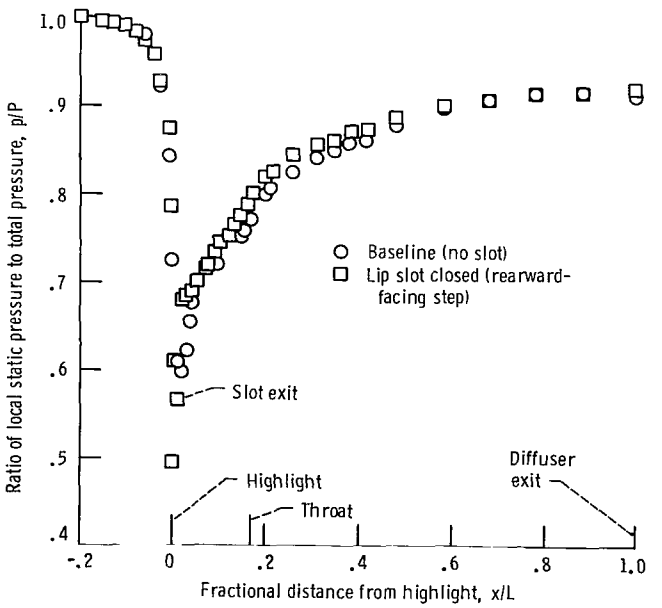

Figure 9. – Effect of lip slot on windward surface static pressure distribution. Lip slot height, h, 0.0508 cm; free-stream velocity, V_0, 18 m/sec; angle of attack, α, 110°.

In contrast to the lip slot the diffuser slot is located downstream of the adverse pressure gradient. At the location where flow reattachment occurs because of the rearward-facing step formed by the diffuser slot, the boundary layer profile probably is not much "weaker" than the profile that exists at this location for the baseline configuration. Both have had to overcome the same adverse pressure gradient shown in figure 9. Thus the diffuser slot would not be expected to have much effect on the inlet flow separation boundary.

Effect of Lip Slot Circumferential Extent

As previously discussed, higher angle-of-attack capability can be achieved by lip blowing than by diffuser blowing. Therefore the remainder of the report presents further details of the aerodynamic performance of the inlet with lip blowing.

The lip blowing results presented so far have been for a slot circumferential extent of 120° (±60° from the windward plane). The effect of changing the lip slot circumferential extent on the flow separation boundary is shown in figure 10. Also shown is the separation boundary for the baseline configuration (dashed line). The results are presented for the smaller lip slot height of 0.0508 cm at a blowing pressure ratio of 1.4. The circumferential extent of the slot was varied by closing the slot so as to minimize the change in the contour of the internal surface near the slot rather than cause a rearward-facing step to occur.

As the figure indicates, a lip slot circumferential extent of greater than 30° was necessary for blowing to be effective. Blowing through a slot circumferential extent of 120° resulted in a very high angle-of-attack capability for the inlet. At V_t/V_0 of 3.0 (which, as already mentioned, is representative of an operating condition that might be encountered during the landing phase of a V/STOL aircraft), the no-slot configuration as well as the inlet with a 30° extent of blowing was capable of achieving an angle of attack of only 55°. Increasing the circumferential extent of blowing to 60° increased the flow separation angle to about 70°; and blowing through a slot circumferential extent of 120° increased the angle-of-attack capability to at least 110°.

The reason for this improvement with increasing circumferential extent of blowing can be explained by examining the circumferential variation of the diffusion velocity ratio shown in figure 11. Diffusion velocity ratio V_{max}/V_{de} is defined as the ratio of maximum to diffuser-exit surface velocities. The results shown in this figure

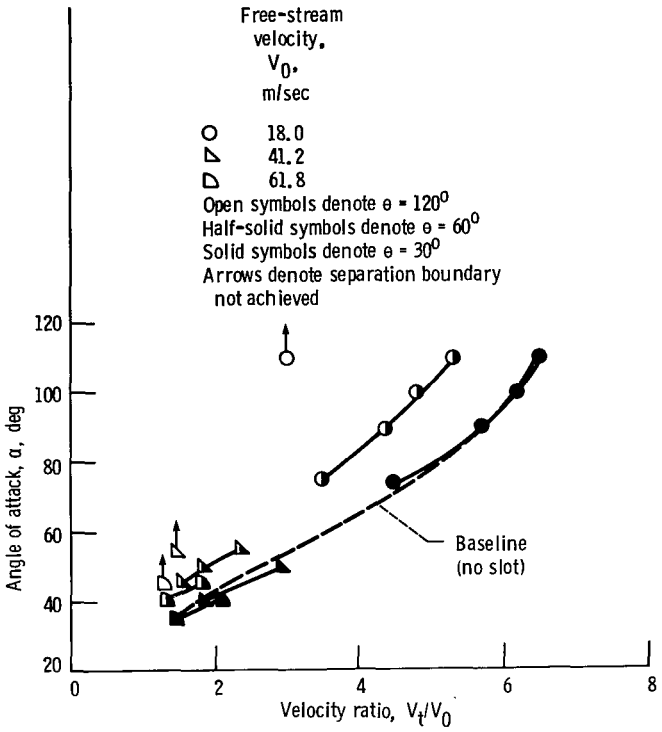

Figure 10. – Effect of lip slot circumferential extent on separation boundary. Lip slot height, h, 0.0508 cm; blowing pressure ratio, P_b/P_0, 1.4.

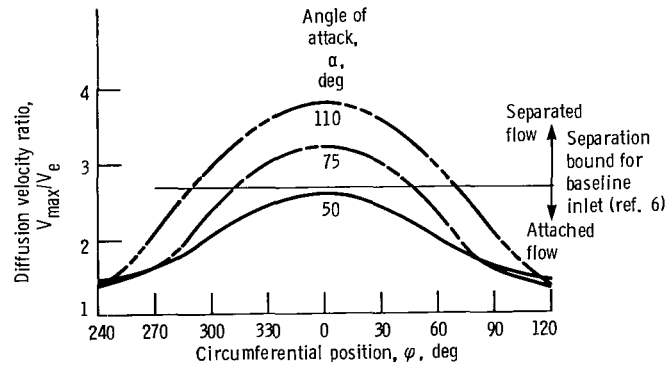

Figure 11. – Analytical circumferential variation of diffusion velocity ratio. Ratio of inlet throat to free-stream velocity, V_t/V_0, 2.5.

were obtained by using the potential flow analysis method described in reference 26. The diffusion velocity ratio parameter can be used as an indicator of whether separation is likely to occur. Previous experimental results (ref. 6) indicated that separation would occur in this inlet when the ratio exceeded a value of about 2.7.

The analytical circumferential variation of the diffusion velocity ratio is shown in figure 11 for three angles of attack at a V_t/V_0 of 2.5. The limiting value of the diffusion velocity ratio, 2.7, is shown in the figure and illustrates that the circumferential extent of the separated region increases with increasing angle of attack. At an angle of attack of 50° no separation would occur since the maximum value of the diffusion velocity ratio was below 2.7. At an angle of attack of 75°, however, separation would occur and the region of separation would extend about 50° on either side of the windward plane ($\varphi = 0°$). At an angle of attack of 110° the region of separation would extend about 70° on either side of the windward plane. Thus, preventing flow separation at high angles of attack requires blowing through a lip slot that has a large circumferential extent. For example, to avoid flow separation at an angle of attack of 110°, the blowing slot would have to extend over at least 120° of the lip circumference.

Effect of Lip Slot Height

The effect of blowing through different lip slot heights on the flow separation boundary is shown in figure 12 for a slot circumferential extent of 120°. At blowing pressure ratios of 1.0 and 1.1 (figs. 12(a) and (b), respectively) blowing through the larger slot ($h = 0.152$ cm, solid symbols) was more effective than blowing through the smaller slot ($h = 0.0508$ cm, open symbols).

This can be explained by examining the boundary layer total pressure profiles shown in figure 13. These profiles are from the diffuser boundary layer rake located just downstream of the throat (fig. 3(a)). Profiles for both slot height configurations are presented for the same conditions (i.e., same values of free-stream velocity, angle of attack, blowing pressure ratio, and throat Mach number). The profile for the baseline configuration is also shown for the same free-stream velocity, angle of attack, and blowing pressure ratio, but for a somewhat lower throat Mach number. Having the same flow conditions for both slot heights (i.e., free-stream velocity and inlet mass flow) means that at any angle of attack the blowing jet velocity was the same. Changing the slot height resulted in changing only the blowing mass flow rate.

For the smaller slot ($h = 0.0508$ cm) the blowing mass flow rate was not sufficient to reenergize the boundary layer. The profile remained essentially the same as that for the baseline inlet.

Increasing the slot height to 0.152 cm tripled the blowing mass flow rate. The mass flow rate tripled because the larger slot area is three times the smaller slot area. This resulted in reenergizing the boundary layer, as shown by the substantial improvement in the total pressure profile. Thus, the increased effectiveness of the larger lip slot height configuration was due to the increase in the blowing mass flow rate.

Comparison of Nonblowing and Lip Blowing

A comparison of the nonblowing and lip blowing results is shown in figure 14. The separation boundary of

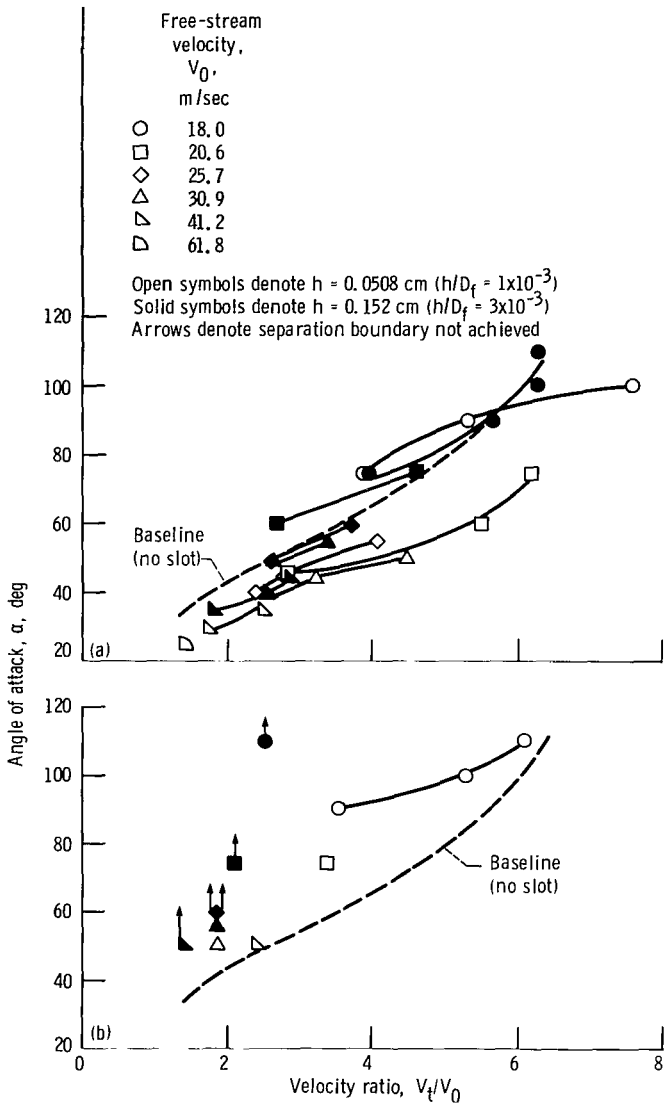

(a) Blowing pressure ratio, P_b/P_0, 1.0.
(b) Blowing pressure ratio, P_b/P_0, 1.1.

Figure 12. – Effect of lip slot height on separation boundary. Circumferential extent of blowing, θ, 120°.

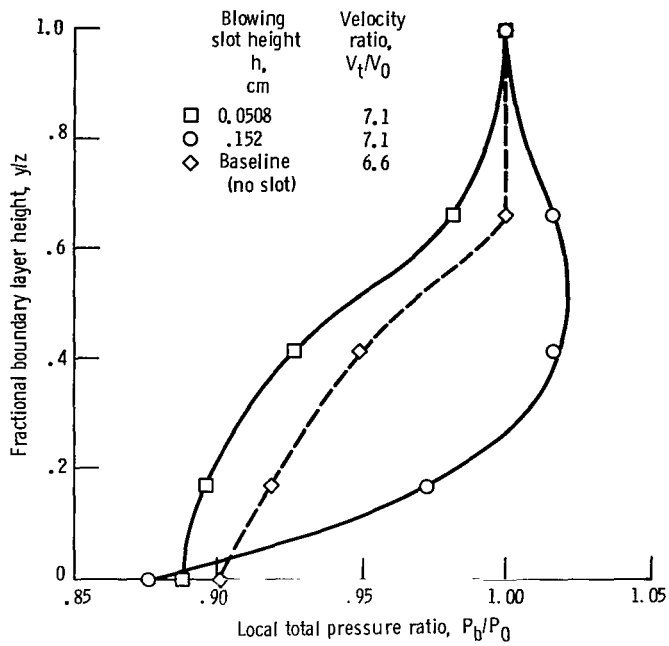

Figure 13. – Effect of lip slot height on diffuser boundary layer profile. Free-stream velocity V_0, 18 m/sec; angle of attack, α, 110°; circumferential extent of blowing, θ, 120°; blowing pressure ratio, P_b/P_0, 1.1; boundary layer rake height, z, 0.526 cm.

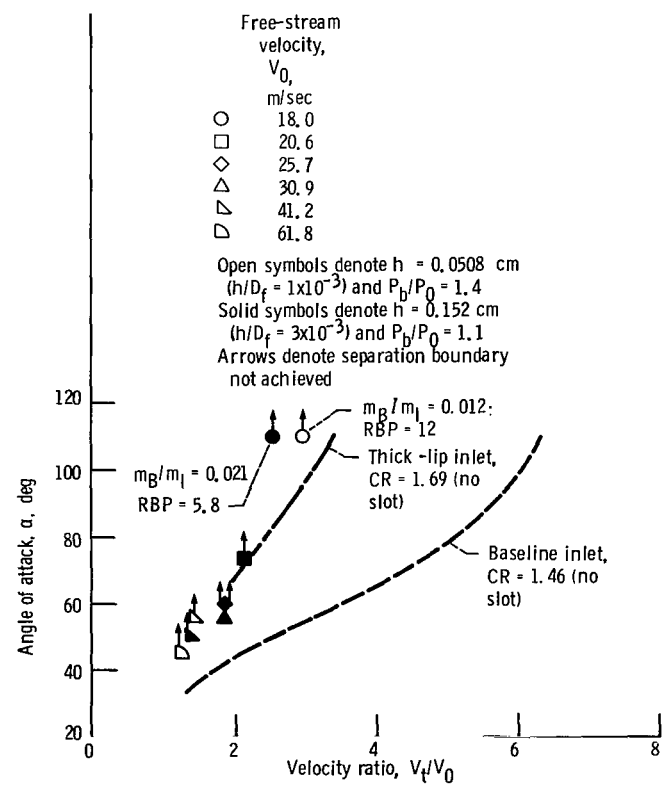

Figure 14. – Comparison of nonblowing and lip blowing. Relative blowing power RBP = $m_b/m_i \times [(P_b/P_0)^{(\gamma-1)/\gamma} - 1] \times 10^4$.

the relatively thin-lip inlet (CR = 1.46) with and without lip blowing is compared with the separation boundary of an inlet having a relatively thick lip (CR = 1.69; ref. 19) and no blowing.

As indicated, lip blowing using the larger slot ($h = 0.152$ cm) at a blowing pressure ratio of 1.1 (solid symbols) can at some conditions double the angle-of-attack capability of the baseline inlet (dashed line). Furthermore this lip blowing configuration is as effective and, in some cases, more effective in achieving high angle-of-attack capability than the thick-lip inlet (dash-dotted line). For example, at a V_t/V_0 of 2.5 the relatively thin-lip baseline inlet was capable of achieving an angle

of attack of only 50°. Lip blowing increased this capability to 110°. By comparison, the thick-lip inlet achieved an angle of attack of 82° at the same velocity ratio of 2.5.

Some Criteria for Selecting Lip Blowing Parameters

The same angle-of-attack capability achieved by blowing through the larger lip slot with a blowing pressure ratio of 1.1 can, of course, also be achieved by blowing through the smaller lip slot. However, to accomplish this requires increasing the blowing pressure ratio to about 1.4, as shown in figure 14 by the open symbols. Since essentially the same angle-of-attack capability can be achieved by blowing through either height lip slot, some criteria are needed to choose between them. One criterion is relative blowing power RBP. The equation used for calculating RBP is shown in figure 14. It is a nondimensional parameter that represents the ratio of the ideal amount of power required to increase the pressure of the blowing air from free-stream total conditions to the desired value P_b divided by the ideal amount of power in the inlet airstream. Note that when the blowing total pressure P_b is equal to the free-stream total pressure P_0, the relative blowing power is zero. This means that ram air can be used as the source of the blowing air and consequently no power from the propulsion system is needed.

The equation also shows that, at the low blowing pressure ratios, blowing power is much more sensitive to changes in blowing pressure ratio than it is to changes in blowing mass flow ratio m_b/m_i. Thus it is more efficient (i.e., requires less power) to reenergize the boundary layer by using a high blowing mass flow ratio at a low blowing pressure ratio than vice versa. On this basis, the larger lip slot height configuration would be chosen. The results shown in the small table in figure 14 confirm this. To achieve the same angle-of-attack capability, the smaller slot required a blowing mass flow ratio of about 0.012 at a blowing pressure ratio of 1.4; the larger slot required a blowing mass flow ratio of about 0.021 at a blowing pressure ratio of 1.1. This resulted in the larger slot requiring only about half the relative blowing power of the smaller slot (5.8 as compared with 12).

Besides relative blowing power, another criterion that could be used to choose between the two lip slot heights is whether the air required for blowing can realistically be bled from the core compressor. According to reference 27 a blowing mass flow ratio of 0.009 and a blowing pressure ratio of 2.6 are well within the bleed capability of a contemporary core compressor. On the basis of this criterion, the smaller lip slot height would be selected. It requires a blowing mass flow ratio of only 0.012 at a blowing pressure ratio of 1.4. The larger mass flow ratio required for blowing through the larger slot (m_b/m_i= 0.021) falls far outside the core-compressor bleed capability reported in reference 27.

However, the low blowing pressure ratio ($P_b/P_0=1.1$) associated with the larger lip slot height raises the possibility that the required air could be bled off downstream of the fan rather than from the core compressor. To achieve this means that, when the fan is throttled back during the landing maneuver, the fan total pressure ratio must stay above a value of 1.1 (at least in the region where the air is bled off). It also implies that, to some extent, the fan operational characteristics are influenced by the separation characteristics of the inlet. Consequently it is probably not possible to use just any fan with this inlet. The fan must be properly matched to the inlet.

Benefit of Lip Blowing

The benefit of lip blowing is that, for a given angle-of-attack capability, the inlet lip can be made thinner. This, in turn, means that the entire inlet can be made thinner and shorter. The effect of this on the overall nacelle design is illustrated in figure 15. The nacelle in figure 15(a) does not use inlet lip blowing. The required angle-of-attack capability is achieved by making the lower lip very thick; this results in a relatively thick, long, and heavy nacelle with relatively large drag at cruise conditions. In contrast, the nacelle with lip blowing (fig. 15(b)) can achieve the same angle-of-attack capability with a much thinner lip. The thinner lip also makes it possible to reduce the nacelle length by shortening the diffuser. The reason is that the thinner lip results in a larger throat area, which means less diffusion length is required. The thinner and shorter inlet results in a lightweight nacelle

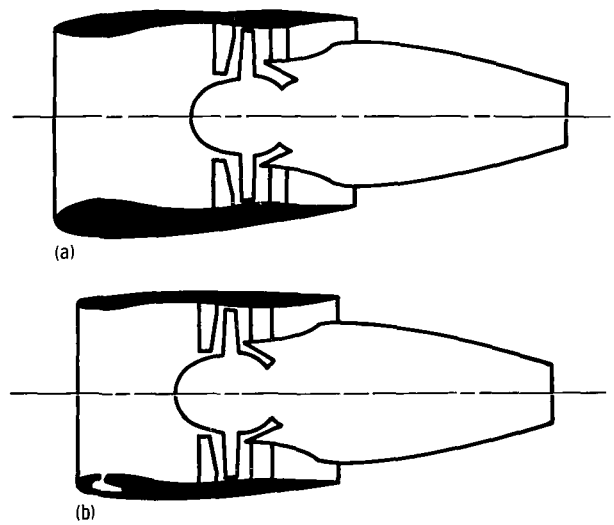

(a) Asymmetric geometry without lip blowing.
(b) Geometry with lip blowing.

Figure 15. – Benefit of blowing.

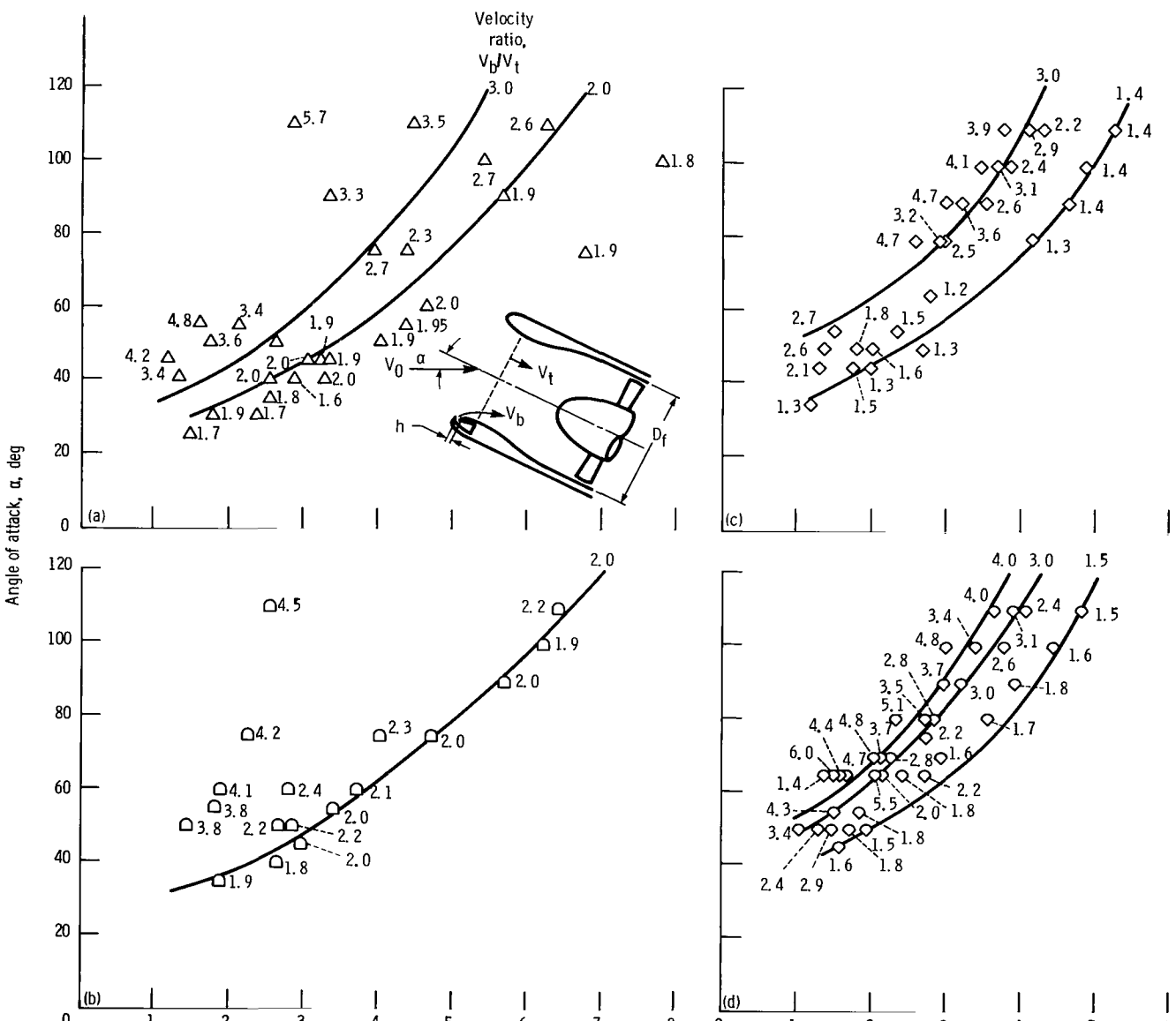

(a) Lip slot height, h, 0.0508 cm.
(b) Lip slot height, h, 0.152 cm.
(c) Diffuser slot height, h, 0.0508 cm.
(d) Diffuser slot height, h, 0.152 cm.

Figure 16. – Correlating parameter for blowing geometry. Circumferential extent of blowing, θ, 120°.

that has lower drag at cruise conditions and thereby increases the payload of subsonic V/STOL aircraft.

There are, of course, penalties associated with the lip blowing system. These would tend to reduce, but not necessarily eliminate, the payload benefit. Weight penalties would be associated with hardware for ducting the blowing air from the engine and also for assuring a highly reliable blowing system. (With the thick lip, there is no question of reliability.) Some thrust penalty would also be assessed the blowing system for using the engine as the air source. These factors, in addition to those presented in this report, must be considered before deciding on whether to use lip blowing to achieve the required angle-of-attack capability.

Blowing Correlating Parameter

The potential correlating parameter to be examined is the ratio of blowing velocity to inlet throat velocity V_b/V_t. It was derived by applying the Buckingham pi theorem for dimensional analysis. The result was that the angle of attack at which flow separation occurred α became a function of four dimensionless parameters:

$$\alpha = f\left(\frac{V_0}{V_t}, \frac{V_b}{V_t}, \frac{1}{\mathrm{Re}_e}, \frac{h}{D_f}\right)$$

By neglecting the Reynolds number effect Re_e and by assuming h/D_f to be constant, the relationship reduces to

$$\alpha = g\left(\frac{V_0}{V_t}, \frac{V_b}{V_t}\right)$$

This relationship must be applied to each blowing geometry since h/D_f is assumed to be constant. For the baseline inlet (i.e., the inlet with no blowing slot), the relationship reduces to

$$\alpha = j\left(\frac{V_0}{V_t}\right)$$

This correlation is shown in figure 6.

How successfully the relationship correlates the blowing results is shown in figure 16 for a slot circumferential extent of 120°. Results are shown in figures 16(a) and (b) for lip slot heights of 0.0508 cm and 0.152 cm, respectively, and in figures 16(c) and (d) for diffuser slot heights of 0.0508 cm and 0.152 cm, respectively. Values of the correlating parameter V_b/V_t range between 1.2 and 5.7. Very few data points have the same value of V_b/V_t because of the procedure for acquiring the data. However, preliminary indications are that the parameter successfully correlates the data, as evident from the lines of constant V_b/V_t drawn through the data for each of the fan geometries. Further investigations, designed specifically to test this correlation, are needed before a final determination of its validity can be made.

Summary of Results

An experimental investigation was conducted to evaluate the effectiveness of tangential blowing in preventing internal flow separation over the range of operating conditions likely to be encountered by inlets for subsonic V/STOL aircraft. The results of the investigation can be summarized as follows:

1. Both lip and diffuser blowing were effective in maintaining attached flow to high angles of attack.
2. Higher angle-of-attack capability was achieved by lip blowing than by diffuser blowing.
3. The angle-of-attack operating range of this inlet was, at some conditions, doubled by lip blowing.
4. Lip blowing was effective with either of the two slot heights. Using the larger lip slot required less power. The boundary layer is more efficiently reenergized by using a high blowing mass flow at a low blowing velocity than by using a low blowing mass flow at a high blowing velocity.
5. Inlet angle-of-attack capability was influenced by the circumferential extent of lip blowing. Lip blowing had to cover a circumferential extent of 120° to maintain attached flow at the highest angles of attack.
6. The ratio of blowing velocity to inlet throat velocity successfully correlated the blowing results for a given blowing geometry (i.e., fixed slot height, location, and circumferential extent).

Lewis Research Center
National Aeronautics and Space Administration
Cleveland, Ohio, December 9, 1983

References

1. Albers, J. A.; and Miller, B. A.: Effect of Subsonic Inlet Lip Geometry on Predicted Surface and Flow Mach Number Distributions. NASA TN D-7446, 1973.
2. Albers, J. A.; Stockman, N. O.; and Hirn, J. J.: Aerodynamic Analysis of Several High Throat Mach Number Inlets for the Quiet Clean Short-Haul Experimental Engine. NASA TM X-3183, 1975.
3. Jakubowski, A. K.; and Luidens, R. W.: Internal Cowl-Separation at High Incidence Angles. AIAA Paper 75-64, Jan. 1975.
4. Miller, B. A.; Dastoli, B. J.; and Wesoky, H. L.: Effect of Entry-Lip Design on Aerodynamics and Acoustics of High Throat Mach Number Inlets for the Quiet Clean, Short-Haul Experimental Engine. NASA TM X-3222, 1975.
5. Luidens, R. W.; and Abbott, J. M.: Incidence Angle Bounds for Lip Flow Separation of Three 13.97-Centimeter-Diameter Inlets. NASA TM X-3351, 1976.
6. Boles, M. A.; and Stockman, N. O.: Use of Experimental Separation Limits in the Theoretical Design of V/STOL Inlets. AIAA Paper 77-878, July 1977.
7. Boles, M. A.; Luidens, R. W.; and Stockman, N. O.: Theoretical Flow Characteristics of Inlets for Tilting-Nacelle VTOL Aircraft. NASA TP-1205, 1978.
8. Hawk, J. D.; and Stockman, N. O.: Theoretical Study of VTOL Tilt-Nacelle Axisymmetric Inlet Geometries. NASA TP-1380, 1979.
9. Burley, R. R.: Effect of Lip and Centerbody Geometry on Aerodynamic Performance of Inlets for Tilting-Nacelle VTOL Aircraft. NASA TM-79056, 1979.
10. Koncsek, J. L.; and Shaw, R. J.: Operating Characteristics of an Inlet Model Tested with a 0.5M Powered Fan at High Angles of Attack. (D180-20798-1, Boeing Co.; NASA Grant NAS3-20597.) NASA CR-135270, 1977.

11. Shaw, R. J.; Williams, R. C.; and Koncsek, J. L.: VSTOL Tilt Nacelle Aerodynamics and Its Relation to Fan Blade Stresses. NASA TM-78899, 1978.
12. Abbott, J. M.: Aeroacoustic Performance of a Scoop Inlet. NASA TM-73725, 1977.
13. Abbott, J. M.; and Dietrich, D. A.: Aerodynamic and Directional Acoustic Performance of a Scoop Inlet. NASA TP-1028, 1977.
14. Abbott, J. M.: Aerodynamic Performance of Scarf Inlets Including Acoustic Advantages. NASA TM-79055, 1979.
15. Miller, B. A.: Inlets for High Angles of Attack. J. Aircr., vol. 13, Apr. 1976, pp. 319-320.
16. Miller, B. A.: Effect of Design Changes on Aerodynamic and Acoustic Performance of Translating Centerbody Sonic Inlets. NASA TP-1132, 1978.
17. Johns, A. L.; Williams, R. C.; and Potonides, H. C.: Performance of a V/STOL Tilt Nacelle Inlet with Blowing Boundary Layer Control. NASA TM-79176, 1979.
18. Lewis, G. W., Jr.; and Tysl, E. R.: Overall and Blade-Element Performance of a 1.20-Pressure-Ratio Fan Stage at Design Blade Setting Angle. NASA TM X-3101, 1974.
19. Potonides, H. C.; Cea, R. A.; and Nelson, T. F.: Design and Experimental Studies of a Type A V/STOL Inlet. J. Aircr., vol. 16, no. 8, Aug. 1979, pp. 543-550.
20. Williams, John; and Butler, Sidney F. J.: Aerodynamic Aspects of Boundary Layer Control for High Lift at Low Speeds. J. R. Aeronaut. Soc., vol. 67, no. 628, Apr. 1963, pp. 201-223.
21. Yuska, J. A.; Diedrich, J. H.; and Clough, N.: Lewis 9- By 15-Foot V/STOL Wind Tunnel. NASA TM X-2305, 1971.
22. Williams, R. C.; Diedrich, J. H.; and Shaw, R. J.: Turbofan Blade Stresses Induced by the Flow Distortion of a VTOL Inlet at High Angles of Attack. NASA TM-82963, 1983.
23. McGregor, I.: Some Applications of Boundary Layer Control by Blowing to Air Inlets for V/STOL Aircraft. Inlets and Nozzles for Aerospace Engines. AGARD CP-91-71, 1971, pp. 12-1 to 12-13.
24. Burley, R. R.; and Hwang, D. P.: Experimental and Analytical Results of Tangential Blowing Applied to a Subsonic V/STOL Inlet. NASA TM-82847, 1982.
25. Chang, P. K.: Separation of Flow. Pergamon Press, 1970, p. 279.
26. Hwang, D. P.: A Summary of V/STOL Inlet Analysis Methods. NASA TM-82725, 1981.
27. Cawthon, J. A.: Design and Preliminary Evaluation of Inlet Concepts Selected for Maneuver Improvements of Transonic Tactical Aircraft. AIAA Paper 76-701, July 1976.

1. Report No.	2. Government Accession No.	3. Recipient's Catalog No.
NASA TP-2297		

4. Title and Subtitle	5. Report Date
Experimental Investigation of Tangential Blowing Applied to a Subsonic V/STOL Inlet	April 1984
	6. Performing Organization Code: 505-43-02

7. Author(s)	8. Performing Organization Report No.
Richard R. Burley	E-1907
	10. Work Unit No.

9. Performing Organization Name and Address	11. Contract or Grant No.
National Aeronautics and Space Administration Lewis Research Center Cleveland, Ohio 44135	
	13. Type of Report and Period Covered: Technical Paper

12. Sponsoring Agency Name and Address	14. Sponsoring Agency Code
National Aeronautics and Space Administration Washington, D.C. 20546	

15. Supplementary Notes

16. Abstract

Engine inlets for subsonic V/STOL aircraft must operate over a wide range of conditions without the severe internal flow separation that can cause sudden changes in engine thrust, excessively high fan blade stresses, and possibly core-compressor stall. An experimental investigation was conducted to evaluate the effectiveness of tangential blowing to maintain attached flow at high inlet angles of attack. The inlet had a relatively thin lip (lip contraction ratio of 1.46). Two blowing slot locations were investigated: one on the lip and the other in the diffuser. The effect of two slot heights (0.0508 and 0.152 cm) and three slot circumferential extents, the largest being 120°, also was investigated. The results showed that both lip and diffuser blowing were effective in maintaining attached flow at high angles of attack. However, higher angle-of-attack capability was achieved with lip blowing than with diffuser blowing. This capability was achieved with the largest slot circumferential extent and either of the two slot heights. The tests were conducted in a low-speed wind tunnel at free-stream velocities between 18 and 62 m/sec and inlet angles of attack to 110°. Inlet throat Mach number varied between 0.15 and 0.60. Blowing pressure ratio (blowing total pressure divided by free-stream total pressure) was varied between 1.0 and 1.4. Blowing temperature ratio (blowing total temperature divided by free-stream total temperature) was nominally 1.0.

17. Key Words (Suggested by Author(s))	18. Distribution Statement
V/STOL inlets Boundary layer control Propulsion	Unclassified - unlimited STAR Category 02

19. Security Classif. (of this report)	20. Security Classif. (of this page)	21. No. of pages	22. Price*
Unclassified	Unclassified	19	A02

*For sale by the National Technical Information Service, Springfield, Virginia 22161

NASA-Langley, 1984

1 1 1U,A, 840402 S00903DS
DEPT OF THE AIR FORCE
AF WEAPONS LABORATORY
ATTN: TECHNICAL LIBRARY (SUL)
KIRTLAND AFB NM 87116